

Effect of Strain Rate and Temperature on Yielding and Fracture Toughness of Brazed Joints of Inconel 718

A power law is suggested that provides a method to estimate plane strain fracture toughness K_{Ic} for any set of strain rates and subroom temperatures

BY B. Z. WEISS AND B. GRUSHKO

ABSTRACT. The effect of strain rate on the yield stress and fracture toughness of the brazed joint was studied at three different temperatures. The brazing filler metal used was BNi5.

Yield-stress/strain-rate dependence was observed at each temperature. It was shown that the yield stress of the brazed joint can be represented as a function of temperature-strain rate. Strain rates at the elasto-plastic boundary ahead of the notch tip were calculated and measured experimentally on two (Charpy V-notch and fatigue precracked) notch geometries. The strain rates measured at the tip of the Charpy V-notch were found to be more than twice lower than those measured at the tip of the fatigue precracked specimens.

The limiting sharpness, ρ_0 , was determined by performing a series of dynamic fracture toughness experiments. In order for microscopic stress criteria for fracture to be applied, the experiments were conducted at -194°C (-317°F). The cleavage strength of the brazed joint was calculated and found to be $\sim 1.8 \text{ GPa}$ ($\sim 180 \text{ kg/mm}^2$ or 261 ksi). The critical plastic zone ranges from $\sim 0.1 \text{ mm}$ (0.004 in.) for highest values of yield stress to 0.25 mm (0.0098 in.) for lowest values of the same stress.

The dependence of fracture toughness on strain rate at different temperatures was also established. A power law was

suggested, which provides a method for estimating the value of K_{Ic} for any set of strain rate and subroom temperature.

Introduction

The penetration of Ni-based superalloys into different fields of modern technology, due to their superior properties, brought with it a problem. This was to find a suitable joining technique that will guarantee the required spectrum of mechanical properties as well as heat and corrosion resistance.

Brazing with Ni-based filler metals, which have replaced the conventional silver alloys and which seem to meet the requirements as to mechanical behavior and heat and corrosion resistance, is probably the best answer to the above mentioned problem of joining. However, some very reactive metals among the Ni-based superalloys are very difficult to reduce and wet only in vacuum or in dry hydrogen. Because of these reactive metals, the brazing of Ni-based superalloys must be carried out in a vacuum ($< \sim 10^{-5} \text{ torr}$) and at high temperature ($> 1075^\circ\text{C}$ or 1967°F).

The brazing filler metals most commonly used in the high-vacuum brazing of Ni-based alloys are multi-component systems whose equilibrium diagrams are only partly known. Therefore, neither the primary nor the secondary phases which appear in the joint after brazing can as a rule be easily predicted.

The BNi5 filler metal used in the present investigation is basically a ternary alloy Ni-Cr-Si (<0.1% C, 70% Ni, 20% Cr, 10% Si, percentages being wt-%).

According to data available from the literature (Ref. 1) for the composition 70% Ni, 20% Cr and 10% Si, the solidus temperature is approximately 1100°C (2012°F), which decreases by at least 30°C (54°F) in the presence of carbon.

The base metal chosen for this study was Inconel 718 (designated N07718 under the Unified Numbering System developed by the Faculty of Automotive Engineers and American Faculty for Testing Materials). This is a superalloy that has good weldability in either the age hardened or the annealed condition (Ref. 2).

Although N07718 may be considered a prime candidate for joining by brazing, some features (such as formation of oxides, wetting problems, and temperature fluctuations) associated with brazing may lead to the development of local discontinuities in the structure. These discontinuities may assume a major importance in achieving the state of crack instability, especially under dynamic loading conditions in strain rate sensitive materials.

Weiss, *et al.* (Ref. 2), showed that at room temperature, a certain dependence of the crack toughness of the BNi5 brazed joint on the strain rate exists; this was not observed in the N07718 base material. The dependence of fracture toughness on strain rate generally indicates dependence of yield stress on strain rate.

In order to obtain more detailed information on the dependence of yield stress and fracture toughness of the brazed joint on strain rate at different temperatures, an appropriate study was undertaken and is reported in this paper.

B. Z. WEISS is Professor and Head and B. GRUSHKO is Assistant, Department of Materials Engineering, Technion, Israel Institute of Technology, Haifa, Israel.

Table 1—Chemical Composition of N07718 Base Metal and BNi5 Filler Metal, Wt-%

	N07718	BNi5
C	0.05	0.1
Cr	8.5	20.0
Ni	53.0	70.0
Mo	3.0	—
Fe	Bal.	—
Al	0.6	—
Ti	0.8	—
Nb/Ta	5.3	—
Si	—	10

Materials, Heat Treatments and Experimental Procedure

The material used in this investigation was a nickel base alloy known under the name of Inconel 718 (designated N07718 throughout this paper) provided by the Rochling Company. Its chemical composition and its mechanical properties in the as-delivered state are given in Tables 1 and 2, respectively. Table 1 also includes the chemical composition of the brazing filler metal.

Brazing was carried out in a high vacuum ($\sim 10^{-5}$ torr) and at temperatures of 1180–1190°C (2156–2174°F). Brazing time was approximately 10 minutes (min). The specimens had been cut parallel with the rolling direction and, after brazing, were cooled to room temperature and then heat treated. The following sequence of heat treatments was introduced after the brazing process.

- Annealing at 1000°C (1832°F) for 10 hours (h) wherein the annealing process was a combination of the homogenization of the brazed joint and a solution treatment.

- Air cooling.

- "Primary" aging for 8 h at 720°C (1328°F), furnace cooling to 620°C (1148°F), and "secondary" aging for a further 8 h.

- Air cooling.

This sequence of heat treatments guaranteed a desirable distribution of the brittle phases in the brazing joint and a relatively small grain growth in the base metal (Ref. 2). Static and dynamic tensile and fracture toughness tests were carried out with a 10 ton dynamic Instron testing machine and with a Tinus Olsen instrumented impact tester. The fracture toughness specimens were tested in three-point bending.

Specimens for measuring parameters describing the crack instability (fracture toughness) are generally fatigue pre-cracked. However, this procedure was abandoned after a few attempts of fatigue pre-cracking of the brazed joints had been made. The fatigue crack propagation, even in side-grooved specimens, could not be controlled. Instead of fatigue pre-cracking, a wire-sharpening procedure was used (Ref. 2).

Table 2—"Static" Mechanical Properties of As-Delivered N07718 Base Metal^(a)

Yield point (0.2% offset), kg/m ² (ksi)	32 (109)
Ultimate tensile strength, kg/m ² (ksi)	79 (269)
Elongation, %	58

(a) Homogenized for 1 h at 955°C (1751°F)

The fracture toughness was calculated from the equation used in fracture mechanics for three-point bending (Ref. 3).

Effect of Strain Rate and Temperature on Brazed Joint Yield Stress Joint

The effect of the strain rate on yielding behavior has for long been of interest to engineering. A variety of techniques has been developed for the study of the effect of the strain rate on yielding phenomena. These techniques involve conventional tensile machines ($\dot{\epsilon} < 10 \text{ s}^{-1}$), tensile impact tests ($\dot{\epsilon} < 10^2 \text{ s}^{-1}$), and the use of explosives ($\dot{\epsilon} > 10^3 \text{ s}^{-1}$). In the range of strain rates obtainable in tensile-impact tests, the yield strength of certain metals and alloys can increase by as much as 200% compared with the yield stress in the "static" test. The yield stress increase is a function of factors (such as structure, chemical composition, grain size, etc.) characterizing the material.

In previous work (Ref. 2), it was shown that the fracture toughness of the brazed joint is strain rate dependent. The dependence of crack toughness on strain rate generally indicates dependence of yield stress on the strain rate. For this reason it was decided to investigate the effect of strain rate on the yield stress (0.2% offset) at three low temperatures—namely, room temperature, -32°C (-26°F) and -194°C (-317°F).

The yield stress was obtained from corresponding strain ($\epsilon_p = 0.002$) measured by means of strain gauges 0.6 mm (0.024 in.) long placed on specially prepared specimens with the brazed joint clearance ~ 1 mm (0.04 in.). The strain rates applied were $\sim 10^{-3} \text{ s}^{-1}$, $\sim 10^{-1} \text{ s}^{-1}$ and $\sim 10^2 \text{ s}^{-1}$.

Dynamic yielding behavior was evaluated by Campbell (Ref. 4) on the basis of the Cottrell-Bilby model for yielding (Ref. 5). This model predicts a power-law relationship for yield strength as a function of strain rate for all those cases where the yielding mechanism involves the breakaway of dislocations from a solute atmosphere. In addition, it predicts a continuously decreasing yield strength with decreasing strain rate instead of a minimum static yield stress as is experimentally observed. This leads to the conclusion that the power-law is applicable only for strain rates above a certain minimum

value and that it may change considerably with the material (Ref. 6).

In multi-phase materials, the yielding mechanisms are much more complex than that based on the Cottrell-Bilby model developed essentially for low-carbon steel. However, the dislocation motion for most of the mechanisms can be thermally activated, as in the solute atmosphere model. For this reason, it is reasonable to assume that the relationship between strain rate and yield stress can be expressed in the form of a power function.

Kendall (Ref. 7) extended these considerations to the range of elevated temperatures in order to check whether the model remains applicable at these temperatures. The experimental results were found to be essentially in agreement with the Cottrell-Bilby model discussed by Campbell (Ref. 4), but slight modifications in the formulation of the model were needed.

A different approach was used by Bennett and Sinclair for describing the low-temperature yield behavior of metals (Ref. 8). They analyzed the behavior on the basis of a simple rate theory. It is generally accepted that in order to characterize the low-temperature yield behavior the following relationship can be used:

$$\dot{\epsilon} = Ae^{-H(\sigma)/RT} \quad (1)$$

where $\dot{\epsilon}$ = strain rate, A = frequency factor, $H(\sigma)$ = stress-modified activation energy, R = gas constant, and T = temperature.

On the basis of the generalized dislocation model, Conrad (Ref. 9) suggested the following relationship between yield stress and apparent activation energy:

$$H = H^* - V\sigma^* \quad (2)$$

where H = apparent activation energy, H^* = apparent activation energy at zero effective stress, σ^* = effective stress, and V = activation volume.

For a constant activation volume, a linear relationship exists between yield stress and apparent activation energy.

When equation (1) is rewritten in logarithmic form, the result is:

$$\ln \dot{\epsilon} = -\frac{H(\sigma)}{RT} + \ln A \quad (3)$$

Equation (3) shows a linearity between $\ln \dot{\epsilon}$ and $1/T$ at constant stress level, i.e., $H(\sigma) = \text{constant}$. The frequency factor A, which has a value of about 10^8 s^{-1} , was found to be independent of stress (Ref. 8). With the frequency factor known, Sinclair and Bennett (Ref. 8) made a point estimate of the apparent activation energy for yielding at any combination of rate and temperature, the particular combinations chosen being those where the yield stress had been determined experimentally. Sinclair and Bennett showed that changes in yield stress may usefully be presented as a function of the so-

called temperature-strain rate parameter $RT \ln A/\dot{\epsilon}$.

Experimental results concerning the dependence of yield stress (0.2% offset) of the brazed joint on strain rate at different testing temperatures are shown in Fig. 1. At each temperature a strain rate dependence, not drastic but still significant, was observed. It must be noted that a number of specimens were tested at each strain rate. However, only results obtained from specimens which on a microscopic level ($\times 30$) showed a flawless fractured surface without porosity, etc., are presented in Fig. 1.

In the impact tensile test, the strain rate (elastic) was determined from the strain history shown by strain gages glued to the specimen. The strain-time ($\epsilon-t$) diagrams were recorded with a memory oscilloscope. The load-time history was recorded simultaneously by a specially devised system which senses the compression loading of the instrumented tup while in contact with the tested specimen—Fig. 2. To avoid any influence of size effect, all tensile specimens were of similar dimensions.

In order to simplify the practical applications of the experimental results for other combinations of strain rates and temperatures, an attempt was made to present the yield stress as a function of the temperature-strain rate parameter introduced by Sinclair and Bennett. Such a representation was successfully used by the author to describe yield stress changes in some other materials with complicated multi-phase structures.

The obtained experimental results were fitted by the least square method in the following relationship, which consists of equation (3) written in a rearranged form:

$$\sigma_y = QRT_0 \left(\frac{T}{T_0} \ln \frac{A}{\dot{\epsilon}} \right)^{-m} \quad (4)$$

where $(T/T_0) \ln (A/\dot{\epsilon})$ is a dimensionless temperature-strain rate parameter; and A = frequency factor taken to be 10^8 s^{-1} , R = gas constant, T_0 = constant solidus temperature of BNi5 assumed to be 1373K (1100°C or 2012°F), Q = constant

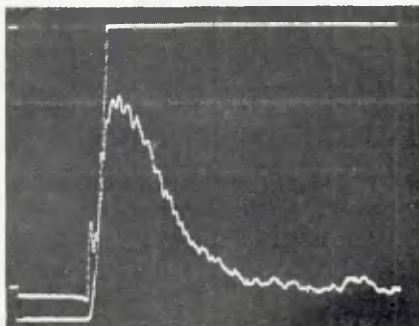


Fig. 2—Oscilloscope traces of the load time and elastic strain-time dependence obtained in a dynamic tensile test. Strain rate $\dot{\epsilon} = 10^2 \text{ s}^{-1}$; load scale $\sim 200 \text{ kg/div}$; time scale $\sim 5 \mu\text{s/div}$

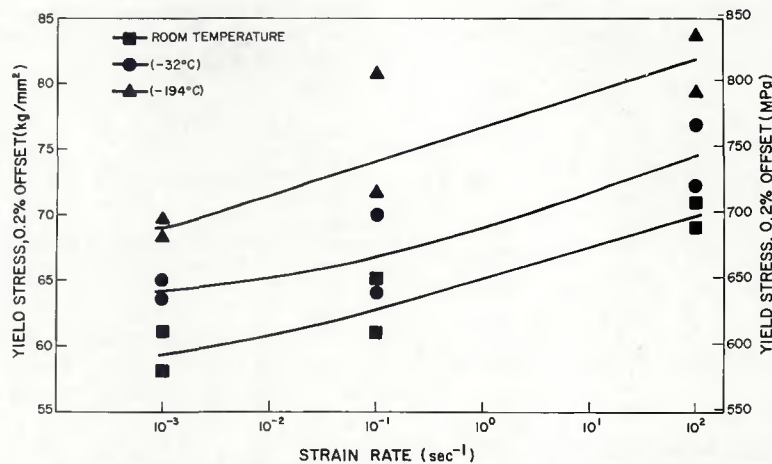


Fig. 1—Dependence of yield stress (0.2% offset) of the brazed joint on strain rate at different testing temperatures

$(Q = 0.0313 \text{ kg mol/cal mm}^2)$, and $m = \text{constant}$ ($m = 0.303$).

The experimental results presented in Fig. 3 show generally small scattering from the correlation function; here there is the tendency of lying above the function for low values of the dimensionless temperature and strain rate parameter and lying below the function for higher values of the parameter. It may, therefore, be concluded that the presented functional correlation can be used for establishing values of yield stress of the brazed joint for different combinations of low temperatures and strain rates. Extension of the suggested correlation to higher temperatures would require more experimental work.

It must also be stated that equation (4) is valid for the brazed joint structure obtained as a result of the sequence of heat treatments described in the previous section. For a different regime of heat treatments, a similar function with probably slightly different constants Q and m might better correlate the experimental results.

Effect of Strain Rate and Temperature on Crack Toughness

The application of linear elastic fracture mechanics to the quantitative evaluation of material performance under loading conditions led to the adoption of the plane-strain fracture toughness (K_{Ic}) as a fully recognized design parameter. Fracture toughness is considered to be a structure-sensitive property; as is common with other properties of this type, it may be strain-rate and temperature dependent.

Most fracture toughness measurements are conducted under static or quasi-static conditions that do not always represent the real situation in the state of crack instability. Even in structures subjected to static loading, high strain rates are liable to occur in microscopic regions in the immediate vicinity of structural discontinuities. Dynamic rather than static characterization of crack instability is, therefore, a better choice for fracture-safe design, especially for strain-rate sensitive materials. According to the data

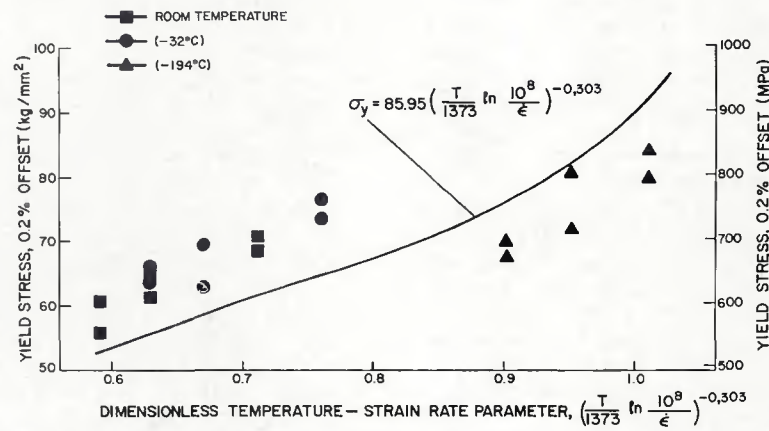


Fig. 3—Yield stress (0.2% offset) of the brazed joint vs. the dimensionless temperature-strain rate parameter

available in the literature, the fracture toughness values K_{Id} (K_{lc} dynamic) are close to the minimum at strain rates obtained from impact tests wherein $\dot{K} = 10^6 \text{ kg mm}^{-3/2} \text{ s}^{-1}$ and \dot{K} is a stress rate intensity parameter (Ref. 10).

In the present section topics associated with crack toughness of the brazed joint are discussed. Results of the investigations of the base metal were published previously, and it was found that the base metal is strain-rate independent (Ref. 2).

Strain Rates at the Tips of Different Notch Geometries

When a notched bar is bent by a dynamically applied load, the material is deformed at the tip of the notch at strain rates that are dependent on the notch geometry. There is no analytical solution for calculating these strain rates, even assuming a purely elastic behavior. The problem is still more complicated when a plastic zone appears ahead of the tip of the notch. Some approximate solutions are known from the literature (Refs. 11-14).

Irwin (Ref. 11) arrived at an estimation of the strain rate at the elasto-plastic boundary of a plastic zone at the crack (notch tip) as being equal to:

$$\dot{\epsilon} = \frac{2\sigma_y}{Et} = \frac{2\sigma_y}{EK} \dot{K} \quad (5)$$

where \dot{K} = stress rate intensity parameter.

Shoemaker and Rolf (Ref. 12) suggested a slightly different expression for the strain rate at the elasto-plastic boundary ahead of the crack tip, namely:

$$\dot{\epsilon} = \frac{2\sqrt{3}\sigma_y}{Et} \quad (6)$$

Hahn and Rosenfield (Ref. 13), looking for a simplified elasto-plastic solution, derived the following expression for the strain rate:

$$\dot{\epsilon} = \frac{10\sigma_y}{EK} \dot{K} \quad (7)$$

Eftis and Krafft (Ref. 14) obtained an estimate of the strain rate at the elasto-plastic boundary near the crack tip by differentiating the equation describing the size of the "process zone":

$$\dot{\epsilon} = \frac{K}{(2\pi d)^{1/2}} = \frac{n\dot{K}}{K} \quad (8)$$

where d = process zone size, and n = strain hardening exponent.

All the solutions presented above are of an approximate nature, and there is no direct way to prove their correctness. All the presented relationships are basically similar and for all practical purposes differ one from the other only by a constant coefficient.

It is apparent that, for strain rate calculations, the yield stress of the material must be known. In other words, in order to define the strain rate for strain-rate sensitive materials, the yield stress at that particular strain rate must be known. Since the brazed joint was found to be strain-rate sensitive, the general expression of yield stress as a function of the temperature strain-rate parameter was used. Combining equation (4) with equation (5) yields:

$$\dot{\epsilon} = \frac{2QRT_0\dot{K}}{EK} \left(\frac{T}{T_0} \ln \frac{A}{\dot{\epsilon}} \right)^{-m} \quad (9)$$

or:

$$\dot{\epsilon} = BQRT_0 \left(\frac{T}{T_0} \right)^{-m} \left(\ln \frac{A}{\dot{\epsilon}} \right)^{-m} \quad (10)$$

or:

$$\dot{\epsilon} = D \left(\ln \frac{A}{\dot{\epsilon}} \right)^{-m} \quad (11)$$

where $B = 2\dot{K}/EK = 2/Et$, $D = BQT/(T/T_0)^{-m}$, $m = 0.303,*$ and $Q = 0.0313.*$

From equation (9) it can be seen that, at constant temperature T , the strain rate $\dot{\epsilon}$ depends either on the time t , or on \dot{K}/K . The interchangeable relationship between t and \dot{K}/K is true on the assumption that the time of load application at the crack tip is the same as that of load application to the specimen.

For a given strain-rate sensitive material it may be expected that changing the notch geometry will lead to differences in load application time, t , at the elasto-plastic boundary near the crack tip. But it is reasonable to assume that for all changes in notch geometries the differences in load application time t will be rather insignificant.

The stress intensity rate parameter \dot{K} was taken from the literature (Ref. 10). For a striking velocity of $\sim 5000 \text{ mm/s}$,

$K \simeq 10^6 \text{ kg mm}^{-3/2} \text{ s}^{-1}$. The critical stress intensity factors were taken to be in the range of 50 to $110 \text{ kg mm}^{-3/2}$ depending on the testing temperature (see next section).

Table 3 presents the calculated values of strain rates at the elasto-plastic boundary according to Irwin (Ref. 11), Shoemaker and Rolfe (Ref. 12) and Hahn and Rosenfield (Ref. 13). Side by side with the calculated results are experimental results obtained at room temperature on specifically prepared specimens with the width of the brazed joint $\sim 1 \text{ mm}$ (0.04 in.).

For the experimental determination of stress rates at the crack tips of impact specimens with different notch geometries (Charpy V-notch and fatigue pre-cracked) the following series of experiments were carried out. Strain gages, each 0.6 mm (0.02 in.) long, were placed at the tips of the two different types of notches, a microscope being used for the operation. The strain gages were glued to both sides of the specimen. All specimens were tested in the instrumented impact machine, and the experimental results, in the form of load vs. time curves and strain vs. time curves taken simultaneously, were recorded on the screen of the oscilloscope.

Figure 4 shows the locations of the strain gauge at the tip of the notch. The recorded results ($\epsilon-t$ and $P-t$) of the impact tests are shown in Figs. 5 and 6. It can be seen from Figs. 5 and 6 that an almost linear dependence between strain, $\dot{\epsilon}$, and time, t , made it easy to establish the values of the elastic strain rates at the tips of the notches existing in the initial stages of the impact test.

When comparing the experimental results for the two notch geometries investigated, Table 3 shows that, under



Fig. 4—Strain rate measurements at the tip of the Charpy V-notch specimen. Strain gage is located at tip of notch. X23 (reduced 50% on reproduction)

Table 3—Calculated and Measured Values of Strain Rates Obtained on Specimens with Different Notch Geometries, s^{-1}

Temperature, K	Irwin (Ref. 11)	Shoemaker and Rolfe (Ref. 12)	Hahn and Rosenfield (Ref. 13)	Measured experimentally ^(a)	
				Charpy	Fatigue precracked
79	$\sim 1.05 \times 10^2$	$\sim 1.85 \times 10^2$	$\sim 5.25 \times 10^2$		
241	$\sim 0.85 \times 10^2$	$\sim 1.5 \times 10^2$	$\sim 4.25 \times 10^2$	2.2×10^2	5.5×10^2
300	$\sim 0.55 \times 10^2$	$\sim 0.95 \times 10^2$	$\sim 2.75 \times 10^2$	2.2×10^2	4.8×10^2
				2.0×10^2	4.4×10^2

(a) For each notch geometry three specimens were tested.

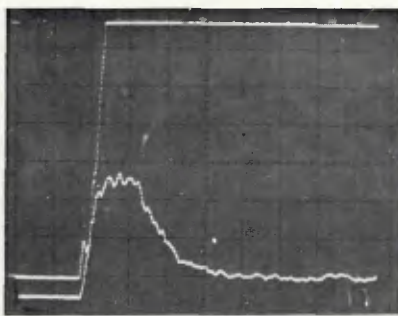


Fig. 5—Oscilloscope traces of the load-time and strain-time dependencies in Charpy specimen tested at room temperature. Strain rate— $\dot{\epsilon} = 2 \times 10^2 \text{ s}^{-1}$; load scale—300 kg/div; time scale—10 $\mu\text{s}/\text{div}$

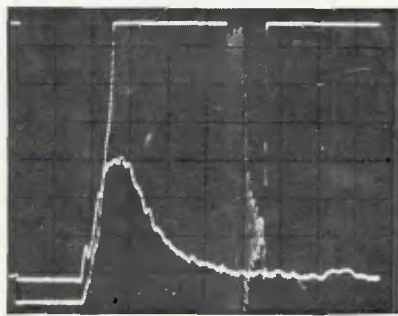


Fig. 6—Oscilloscope traces of the load-time and strain-time dependencies in fatigue pre-cracked specimen tested at room temperature. Strain rate— $\dot{\epsilon} = 5 \times 10^2 \text{ s}^{-1}$; load scale—200 kg/div; time scale—10 $\mu\text{s}/\text{div}$

identical loading conditions, the strain rates obtained at the tips of precracked specimens of the brazed joint are more than twice as high as rates at the tip of the Charpy V-notch. When comparing results obtained experimentally with those calculated, Table 3 indicates that the results predicted by Hahn and Rosenfield were found to be closest to those measured experimentally on fatigue pre-cracked specimens.

Fracture Toughness and the Notch Root Radius-Limiting Sharpness

The critical value of the crack tip opening displacement depends on what occurs at the crack tip. In strain rate sensitive materials, the introduction of a notch or the appearance of a crack may accelerate the attainment of quasi-brittle or brittle behavior during loading primarily due to an increased effective strain rate at the tip, which raises the yield stress.

In the brittle or quasi-brittle range of behavior it can be assumed that the crack begins to propagate when the local tensile stress reaches the cleavage strength σ_f^* .

It has been shown (Ref. 15) that the microscopic cleavage strength σ_f^* can be related to the macroscopic fracture toughness K_{Ic} by comparing the value of the critical plastic zone size R_f expressed by microscopic cleavage strength on the

one hand with the fracture toughness, K_{Ic} , on the other hand:

$$R_f = \left[\exp\left(\frac{\sigma_f^*}{\sigma_y} - 1\right) \rho \right] = 0.12 \left(\frac{K_{Ic}}{\sigma_y} \right)^2 \quad (12)$$

where ρ = radius of the crack (notch tip).

Rearranging yields:

$$K_{Ic}(\rho) = 2.9 \sigma_y \left[\exp\left(\frac{\sigma_f^*}{\sigma_y} - 1\right) - 1 \right]^{1/2} \sqrt{\rho} \quad (13)$$

According to equation (13), the fracture toughness decreases with the decrease in the root radius of the notch tip. Experimentally, it was shown that the crack toughness decreases until some critical root radius ρ_o , called limiting sharpness, is reached. The ρ_o value permits determination of the size of the "process zone" ahead of the crack, over which the σ_f^* must be achieved in order to initiate unstable fracture.

Information on ρ_o is of importance from two points of view:

1. It permits the establishment of the minimum value of K_{Ic} for sharp flows.
2. It is a means for establishing the

minimal sharpness of a flow below which the effect of root radius on fracture toughness is no longer valid.

The limiting sharpness ρ_o can be determined experimentally by performing a series of fracture toughness experiments at a temperature at which the microscopic stress criteria for fracture may be applied. The most convenient way is to use small impact specimens with different notch root radii. Experiments were accordingly carried out on a series of specially prepared brazed samples, the width of the brazed joint (i.e., joint clearance) being up to 2 mm (0.08 in.). Charpy-like impact specimens, with notches having different tip radii machined in the brazing, were prepared. For small radii, the final process was wire sharpening. The impact experiments for fracture toughness determination were carried out at -194°C (-317°F). The results were presented in Fig. 7. It can be seen that the limiting sharpness for the brazing material BNi5 was found to be $\rho_o \approx 0.04 \text{ mm}$ (0.0016 in.).

Bearing in mind that the limiting sharp-

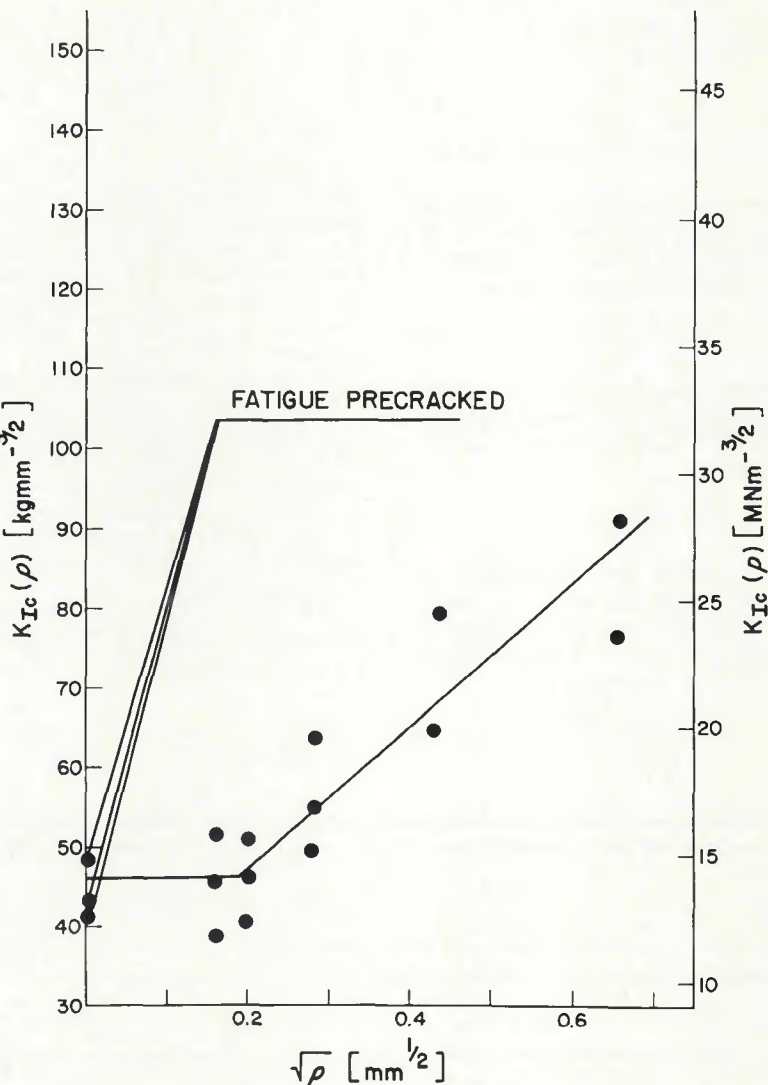


Fig. 7—Dependence of fracture toughness of braze on the radius of the tip of the notch

ness is independent of temperature and strain rate, the information obtained is of experimental importance. When fatigue testing facilities for the precracking purposes are not available or the fatigue crack propagation cannot be controlled, a wire of radius $\rho < 0.04$ mm (0.0016 in.) may be used for sharpening the notch (Ref. 2). Fracture toughness experiments carried out with such specimens will give valid K_{Ic} values, if certain other requirements are fulfilled. The radius ρ_o may depend to some extent on certain microstructural properties of the material, i.e., grain size, impurities, etc.

Since the limiting sharpness is temperature and strain rate independent, the K_{Ic} (ρ_o) will depend only on yield stress σ_y —see equation (13). With K_{Ic} (ρ_o) and ρ_o values experimentally determined (see Fig. 7) for a specific strain rate and temperature and with the yield stress σ_y for the same conditions known (see Fig. 3), the cleavage strength σ_f^* may be calculated (Ref. 15).

By using this procedure it was found that the cleavage strength σ_f^* for the brazing is equal to ~ 180 kg/mm² (~ 1.8 GPa, i.e., 1800 MPa or 261 ksi). When σ_f^* and ρ_o , which are both practically strain rate and temperature independent, are introduced into equation (12), it can be seen that the "process zone" (critical plastic zone size) R_f is only dependent on yield stress σ_y . Substituting for σ_y values established experimentally and shown in Fig. 1, it was found that the R_f ranges from ~ 0.1 mm (0.004 in.) for highest values of σ_y (~ 80 kg/mm², i.e., 116 ksi) to 0.25 mm (0.01 in.) for the lowest values of σ_y (~ 60 kg/mm², i.e., 87 ksi).

Effect of Strain Rate and Temperature on the Fracture Toughness of the Brazed Joint

In the previous work by Weiss, et al. (Ref. 2), it was shown that (although at room temperature fracture toughness of Inconel 718 is strain rate independent) the dependence of the brazing joint (BNi5) on strain rate at that temperature was well established. It would, therefore, be useful to:

1. Evaluate the dependence of crack toughness on the strain rate at different temperatures.

2. Develop a relationship which will provide a method for estimating the value of K_{Ic} under given conditions if it is known for another set of conditions (ignoring environmental effects).

Such an approach, which is based on the relationship between K_{Ic} and strain-rate-dependent mechanical properties, was suggested by Hahn, et al. (Ref. 16), and is given in a general form by equation (14):

$$\frac{\sigma_f^*}{\sigma_y} = f\left(\frac{K_{Ic}}{\sigma_y}\right) \quad (14)$$

Since σ_f^* is generally independent of temperature and strain rate, changes in K_{Ic} should depend only on yield stress, σ_y . It was found (Ref. 16) that a power law describes the relationship in the most suitable way:

$$\frac{\sigma_f^*}{\sigma_y} = \gamma \left(\frac{K_{Ic}}{\sigma_y}\right)^\beta \quad (15)$$

where γ and β constants differ for different materials.

After rearrangement, equation (15) may be written:

$$\sigma_f^* \gamma^{-1} = K_{Ic}^\beta \sigma_y^{1-\beta} \quad (16)$$

Since σ_f^* is temperature independent, the right-hand side of equation (16) should also be independent of temperature, provided the appropriate value of σ_y is used.

It should be pointed out that $K_{Ic}^\beta \sigma_y^{1-\beta}$ is constant and valid only for cleavage fracture. For mixed mode fracture (shear and cleavage) or ductile fracture (shear), the relationship shown by equation (16) is not valid. With decreasing temperature, σ_y increases and K_{Ic} should decrease; for increasing temperature, an opposite effect should be observed.

Substituting, for σ_y in equation (4) and the calculated value of 180 kg/mm² (~ 1.8 GPa, i.e., 261 ksi) for σ_f^* , the K_{Ic} value can be expressed for any set of strain rates and temperatures by equation (17), provided the γ and β constants are known:

$$180\gamma^{-1} \left[85.95 \left(\frac{T}{1373} \ln \frac{10^8}{\epsilon} \right)^{\beta-1} \right] = K_{Ic}^\beta \quad (17)$$

The fracture toughness experiments at strain rates $\dot{\epsilon} \approx 10^{-3}$ s⁻¹ and $\dot{\epsilon} \approx 10^{-1}$ s⁻¹ were carried out in three-point bending on a 10 ton Instron testing machine. The crack toughness was evaluated by means of load (COD) vs. time diagrams. The measurements at $\dot{\epsilon} \approx 10^2$ s⁻¹ were made with the instrumented impact machine, and the fracture toughness was determined from the load-time curves recorded during the impact. Since the load-time dependence in the specimens of the brazed joint was basically linear until fracture, the crack toughness was determined by using linear fracture mechanics (LEFM) considerations.

The procedure for determining the fracture toughness was the same regardless of the strain rate at which the specimens were tested. The strain rate at each loading condition was obtained from the strain vs. time curve recorded by means of a pair of strain gauges glued to both sides of the specimen on the level of the presawed notch and taken simultaneously with the load vs. time curve. The strain rate so measured could be directly related to the external dynamic loading. It is obvious that the elastic strain rates at the tip of the presawed notch are much higher.

At lower strain rates ($\dot{\epsilon} \approx 10^{-3}$ s⁻¹ and $\dot{\epsilon} \approx 10^{-1}$ s⁻¹) the fracture toughness experiments were carried out at two sub-zero temperatures—namely -32 and -60°C (-26 and -76°F). The specimens during the test were practically submerged inside the coolant. At strain rates $\dot{\epsilon} \approx 10^2$ s⁻¹, the applied temperatures were -32 , -60 and -194°C (-26 , -76 , and -317°F).

Figure 8 shows experimental results of crack toughness at different testing temperatures as a function of strain rate. Results at room temperature were taken from the literature (Ref. 2).

The obtained experimental results were fitted by the least square method to

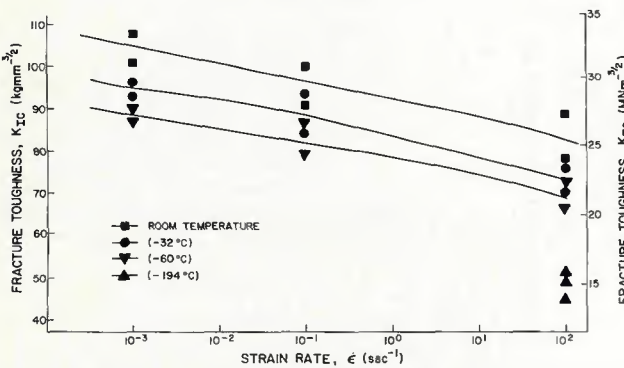


Fig. 8—Crack toughness of braze at different testing temperature as a function of strain rate

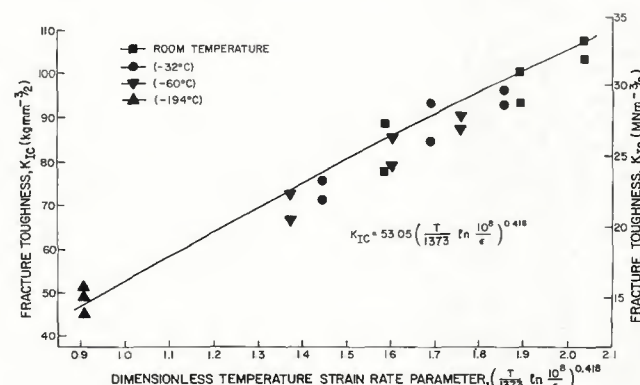


Fig. 9—Functional dependence between the fracture toughness K_{Ic} of the braze and the dimensionless temperature-strain rate parameter

equation (17), yielding the following functional dependence between the fracture toughness K_{Ic} and the strain rate and temperature (temperature-strain-rate parameter):

$$K_{Ic} = 53.05 \left(\frac{T}{1373} \ln \frac{10^8}{\dot{\epsilon}} \right)^{0.418} \quad (18)$$

(γ and β were found to be 2.56 and 0.42 respectively).

Figure 9 shows scattering of the experimental results from the calculated curve—equation (18). The fit of the results is very good, and it may be concluded that, similar to the yield stress, the fracture toughness K_{Ic} can also be presented as a function of the temperature-strain-rate parameter.

Equation (18) is structure-dependent and, in the present case, is valid only for a microstructure resulting from the brazing process and a set of post-brazing heat treatments described in one of the preceding sections. Alteration of the microstructure may slightly change the constants α and β , but the general form of equation (18) will be probably preserved.

All the results reported in Fig. 8 were obtained below room temperature. Extension of equation (18) to higher temperatures will require further experimental confirmation.

The time-load dependence in the brazed joint specimens at all applied strain rates is practically linear until fracture occurs. The double cantilever beam clip gauge used at lower strain rates for recording COD vs. time is not sensitive enough to register prefracture cracking of brittle particles; this may occur during early stages of loading, well before the load reaches its maximum value.

Only when the cracks have propagated substantially does the COD curve show a discontinuous change in slope, which may appear especially at higher strain rates before the maximum load is reached—see Fig. 10. In the high strain-rate (impact) experiments, discontinuities

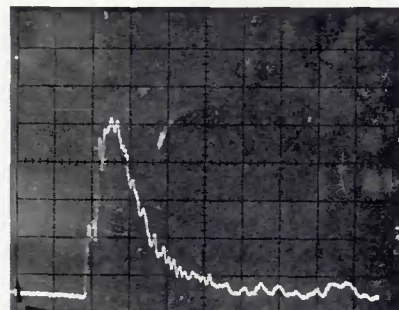


Fig. 11—Discontinuities at the load-time curve above the first inertia peak caused by crack formation and propagation in the brittle phases inside the braze

in the load-time curve above the first inertia peak (Fig. 11) may probably be attributed to pre-fracture crack formation and propagation in the brittle phases inside the braze. These cracks may be arrested for a short time by the surrounding ductile matrix until, in fact, the load reaches the level characteristic for crack instability.

Summary

The effect of strain rate on the yield stress and fracture toughness of the brazed joint was studied at three different subroom temperatures. The brazing filler metal used was BNi5. In order to achieve a desirable distribution of the brittle phases in the brazed joint and to avoid intensive grain growth in the base metal, the following sequence of heat treatments was chosen after the brazing process:

1. Homogenization at 1100°C (2012°F) for 10 h.
2. Air cooling.
3. Aging for 8 h at 720°C (1328°F).
4. Furnace cooling to 620°C (1148°F).
5. Aging for an additional 8 h followed by air cooling.

This sequence of heat treatments not only guaranteed a least deleterious distri-

bution of the brittle phases in the brazed joint, but also caused relatively small grain growth in the base material.

Significant (but not drastic) yield-stress/strain-rate dependence was observed at each temperature. It was shown that the yield stress of the brazed joint can be represented as a function of a dimensionless temperature-strain rate parameter. The experimental results show rather small scattering from the correlation function. The function presented can be used for establishing values of yield stress for different combinations of low-subroom temperatures and strain rates. Extension of the suggested correlation to higher temperatures requires more experimental evidence. Strain rates at the elastoplastic boundary ahead of the notch tip were calculated and measured experimentally by means of strain gages in the case of two (Charpy V-notch and fatigue precracked) notch geometries.

Experimental results have shown that under identical loading conditions the strain rates measured at the tip of fatigue precracked specimens are more than twice as high as those measured at the tip of the Charpy V-notch. The theoretical results predicted by Hahn and Rosenfield were found to be closest to those measured experimentally on fatigue pre-cracked specimens.

The limiting sharpness, ρ_0 , was determined by performing a series of dynamic fracture toughness experiments on specimens with different notch root radii. In order that microscopic stress criterion for fracture could be applied, the experiments were conducted at -194°C (-317°F). The limiting sharpness of brazing was found to be $\rho_0 \approx 0.04$ mm (0.0016 in.).

The cleavage strength was calculated to be ~180 Kg/mm² (~1.8 GPa or 261 ksi). The critical plastic zone ranges from ~0.1 mm (0.004 in.) for highest values of yield stress to 0.25 mm (0.0098 in.) for lowest values of the same stress.

The dependence of fracture toughness of the brazed joint on strain rate at different temperatures was also established. A power law was suggested that provides a method for estimating the value of K_{Ic} for any set of strain rates and subroom temperatures.

Acknowledgment

The authors are deeply indebted to Professor H.D. Steffens and Dr. B. Wielage for fruitful suggestions, help and critical discussions during the performance of this research. The financial support of the Deutsche Forschungsgemeinschaft is greatly appreciated.

References

1. Gray, I., and Miller, G. P. 1964. *Jour. Inst. Met.* 93: 315.
2. Weiss, B. Z., Steffens, H. D., Engelhart, A. H., and Wielage, B. 1979. Static and dynamic crack toughness of brazed joints of Inconel

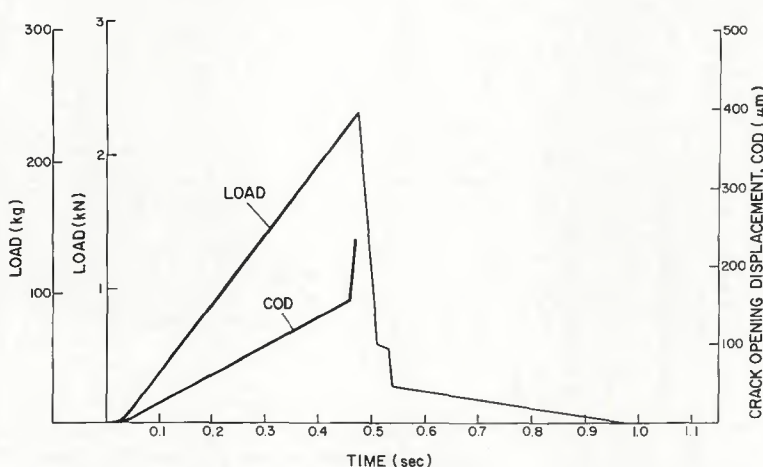


Fig. 10—Load, crack opening displacement in brazing as a function of time. Specimen tested at -60°C (-76°F) at strain rate $\dot{\epsilon} = 10^{-1} \text{ s}^{-1}$

- 718 nickel-base alloy. *Welding Journal* 58(10): 287-s to 295-s.
3. Brown, W. F., and Strawley, E. J. 1966. Plain strain crack toughness testing of high strength metallic materials. *ASTM special technical publication no. 410*.
 4. Campbell, J. D. 1953. The dynamic yielding of mild steel. *Acta Met.* 1: 706.
 5. Cottrell A. H., and Bilby, B. A. 1969. *Proc. Phys. Soc. A62*, 49.
 6. Kendall, D. P., and Davidson, T. E. 1966. The effect of strain rate on yielding in high strength steels. *Trans. ASME series D*, 88, 37.
 7. Kendall, D. P. 1972. The effect of strain rate and temperature on yielding in steels. *Jour. Basic Engng* 94: 207. (Trans. ASME.)
 8. Bennett, P. E., and Sinclair, G. M. 1966. Parameter representation of low-temperature yield behaviour of body-centered cubic transition metals. *Jour. Basic Engng* 88:518. (Trans. ASME.)
 9. Conrad, H. 1961. On the mechanism of yielding and flow in iron. *JSI* 198:364.
 10. Schmidmann, E., and Scherber, H., 1973. The effect of strain rate on the characteristic value of the linear-elastic fracture mechanics determined on large and small specimens. *Materialprüfung* 15:73.
 11. Irwin, G. R. 1964. Crack toughness testing of strain rate sensitive materials. *Jour. Engng for Power* (ASME A86):444.
 12. Shoemaker, A. K., and Rolfe, S. T. 1969. Static and dynamic low-temperature K_{Ic} behaviour of steels. *Jour. Basic Engng* 91:512.
 13. Rosenfield, A. R., and Hahn, G. T. 1966. Numerical description of ambient low-temperature and high strain rate flow and fracture behaviour of plain carbon steel. *Trans. ASM* 59:963.
 14. Eftis, J., and Krafft, J. M. 1965. A comparison of the initiation with the rapid propagation of cracks in mild steel. *Trans. ASME (B)* 187:257.
 15. Teterman, A. S., and McEvily, A. J. 1967. Fracture of structural materials. New York: John Wiley.
 16. Hahn, G. T., Hoagland, and Rosenfield, A. R. 1971. The variations of K_{Ic} with temperature and loading rate. *Met. Trans.* 2:537.

WRC Bulletin 284 April, 1983

The External Pressure Collapse Tests of Tubes

by E. Tschoope and J. R. Maison

An experimental program was performed to confirm or refute the applicability of Figure UG-31 in Section VIII, Division 1 of the ASME Boiler and Pressure Vessel Code to the design of tubes under external pressure. Commercially available tubes were subjected to external pressure until collapse occurred. The data generated indicates the current ASME design rules for tubes under external pressure are suitable for continued application.

Publication of this report was sponsored by the Subcommittee on Shells of the Pressure Vessel Research Committee of the Welding Research Council.

The price of WRC Bulletin 284 is \$12.00 per copy, plus \$5.00 for postage and handling. Orders should be sent with payment to the Welding Research Council, Room 1301, 345 East 47th St., New York, NY 10017.

WRC Bulletin 283 February, 1983

A Critical Evaluation of Fatigue Crack Growth Measurement Techniques for Elevated Temperature Applications by A. E. Carden

The report contains a discussion and evaluation of several crack length measurement techniques at elevated temperature and presents results from the experimental technique developed at the University of Alabama.

Publication of this report was sponsored by the Subcommittee on Cyclic and Creep Behavior of Components of the Pressure Vessel Research Committee of the Welding Research Council.

The price of WRC Bulletin 283 is \$12.00 per copy, plus \$5.00 for postage and handling (foreign + \$8.00). Orders should be sent with payment to the Welding Research Council, 345 East 47th St., Room 1301, New York, NY 10017.